J Mater Sci (2011) 46:4964–4970
DOI 10.1007/s10853-011-5413-z

Effect of additives on the morphology of single-crystal Au nanosheet synthesized using the polyol process

Jinting Jiu · Katsuaki Suganuma · Masaya Nogi

Received: 25 October 2010 / Accepted: 18 February 2011 / Published online: 1 March 2011

Abstract Triangular and hexagonal-shaped single-crystal Au nanosheets were prepared by the reduction of $HAuCl_4$ with the polyol method, after addition of a polyvinylpyrolidone (PVP) capping agent and salts. Both capping agent and salts played a crucial role during nanosheet growth. The high PVP concentration was found to result in a mixed Au morphology of sheets and spherical particles, which could be tailored with the addition of salts to provide solely nanosheets. The main product is always nanosheets after the salts have been added. The selective adsorption of PVP and salt ions onto certain crystallographic facets is thought to be important in the proposed growth mechanism. This synthetic route is simple and fast, and can be extended to other morphology metal particles with careful salt and capping agent selection.

Introduction

Much effort has recently been given to synthesize nanostructured metals because of their potential in applications including catalysis, photochemistry, sensors, and the nanofabrication of electronic, optical and magnetic devices [1–4]. Ag and Au nanosheets have attracted much attention because they offer new possibilities for fundamental studies and applications [5–8]. Various methods have been developed for preparing spherical metal nanoparticles. The production of shape controlled nanostructures remains a challenge for which there is great interest in developing new methods [9–11].

J. Jiu (✉) · K. Suganuma · M. Nogi
Institute of Scientific and Industrial Research, Osaka University, Osaka 567-0047, Japan
e-mail: jiujinting@hotmail.com; jiu@eco.sanken.osaka-u.ac.jp

Nanostructured metals have generally been obtained by one of two different approaches. Surfactants and polymers can act as capping reagents at the surface of metal nanoparticles, and can induce anisotropic growth of different planes [12, 13]. Another approach is templated reactions such as self- or induced assembly of surfactants, block copolymers, and mesoporous solids [10, 14, 15]. Processes involving solution-based polyols modified with capping agents are attractive because of their simplicity and compatibility in open air environments. This process was first reported by Figlarz et al. in 1989 for the preparation of mono-disperse metal nanoparticles [16]. This method was recently used to fabricate mono-disperse single-crystal Ag and Au nanocubes using polyvinylpyrolidone (PVP) as the protecting agent and ethylene glycol (EG) as the reductant and solvent [13]. Tsuji et al. reported the preparation of Au plates by the polyol process using microwave heating. Unsatisfactory shape control was apparent and the product was a mixture of nanoplates and square/spherical particles [17]. Li et al. [18] synthesized single-crystal Au nanosheets using the polyol process with aqueous $HAuCl_4$ in the absence of air and light, and discussed the formation mechanism. They concluded that formation was attributed to the preferential adsorption of molecular species on (111) planes of Au nuclei, leading to small triangular and truncated triangular (or hexagonal) nanosheets.

Other groups have found that product morphology from the polyol process was greatly affected by contaminant traces such as ionic species. Xia et al. suggested that trace amounts of Fe(II) or Fe(III) drastically affected the yield and shape of Ag nanorods, by removing oxygen from the Ag seed surface and preventing dissolution by oxidative etching [19]. Single-crystal cubes and tetrahedrons of Ag with truncated corners have been prepared in high yield using trace sodium chloride in the polyol process by the

same group. A wet etching mechanism was proposed, in which the addition of Cl^- resulted in enhanced oxidation and preferential etching of twinned Ag nuclei, leaving only single crystalline particles to grow into nanoscale cubes and tetrahedrons [20]. Our group has also synthesized Ag nanorods from various salt additives, and discussed their growth mechanism using the polyol process [21]. We found that the morphology and yield of Ag particles depended on the additive. Trace amount of additives have also been shown to control the growth direction of other noble metals, including Pt [22]. These results suggested that careful selection of additive in the polyol process, may allow the preparation of metal nanoparticles with different morphologies. The exact role of trace species in this process remains unclear, and further work with other additives and metal nanoparticles is needed for understanding the polyol process mechanism.

In the current study, we report the large-scale synthesis of micron-sized Au nanosheets, using the polyol process with the addition of trace inorganic salts, such as $FeCl_3$, NaCl, and $CuCl_2$. We have investigated the relationship between salt and product morphology. $HAuCl_4$ was selected as the Au source and was reduced by ethylene glycol (EG), which also acted as the solvent. Polyvinylpyrolidone (PVP, M_W 360 k) is soluble in EG and was used as a protecting and dispersing agent to avoid aggregation of the Au nanoparticles. Trace salts were used to improve the resulting nanoparticle morphology, and their growth mechanism is discussed.

Experimental

In a standard synthesis, 33 mg of $HAuCl_4 \cdot 3H_2O$ and 21 mg of PVP were dissolved in 12 mL of EG at room temperature, to form a transparent yellow solution. This was heated to 150 °C in the ambient atmosphere and held at this temperature for one to several hours to prepare the Au nanoparticles. The reaction could be easily followed using its distinctive color changes. The initial yellow solution (due to $AuCl_4^-$) became lighter until eventually colorless, indicating the formation of Au nanoparticles. The resulting solution was diluted with a large volume of acetone and ethanol, and Au particles were collected by centrifugation at 4,000 rpm for 5 min. This allowed the removal of the PVP capping agent and organic by-products. To elucidate the effect of salts on morphology, $FeCl_3$ and other salts were dissolved in EG and added to the initial yellow solution at room temperature. Au particles were characterized by scanning electron microscopy (SEM; JEOL, JSM-5510S). X-ray powder diffraction (XRD) patterns were recorded using a Rigaku RINT 2500 diffractometer with Cu Kα radiation over a 2θ range of 20–80°. For XRD analysis, samples precipitated in ethanol were deposited onto a glass substrate to form a thin film. A drop this solution was also deposited onto a carbon film grid, and examined using transmission electron microscopy (TEM; JEOL 200CX).

Results and discussion

Figure 1a shows a SEM image of the product obtained from heating 33 mg of $HAuCl_4 \cdot 3H_2O$ in 12 mL of EG with 21 mg of PVP capping agent for 1 h at 150 °C, with 32 μM of $FeCl_3$. Large Au nanosheets greater than 30 μm long and some smaller sheets were formed. The SEM images (Fig. 1a, b) show that the products were mainly Au sheets of equilateral or truncated triangles and hexagonal shapes. This is similar to results reported by Zhang et al., where the same method was used with significantly more capping agent, in the absence of salt and at a lower reaction temperature [18].

The XRD pattern of the product is shown in Fig. 2. The four apparent peaks were assigned to diffractions from

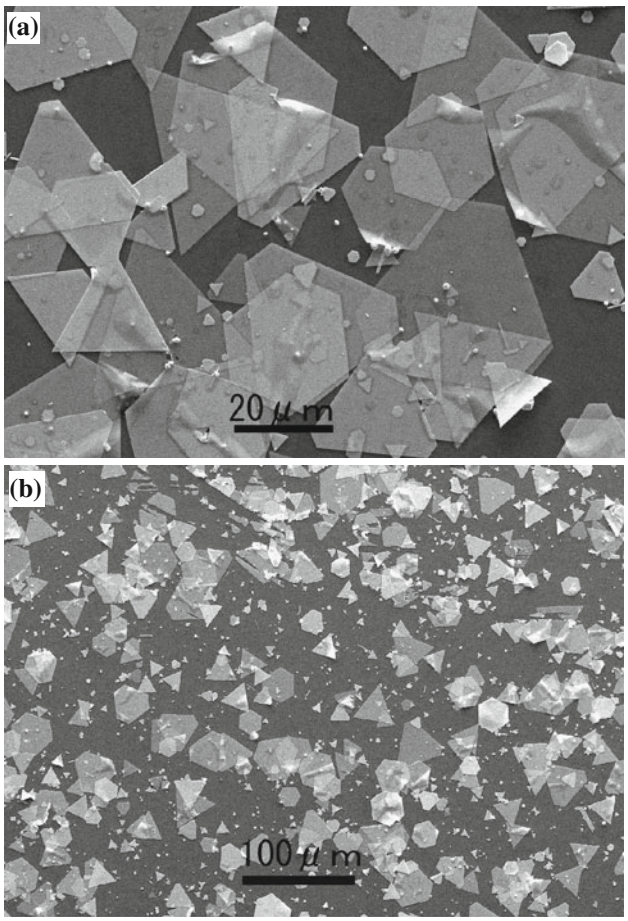

Fig. 1 High magnification (**a**) and low magnification (**b**) SEM images of the precipitate

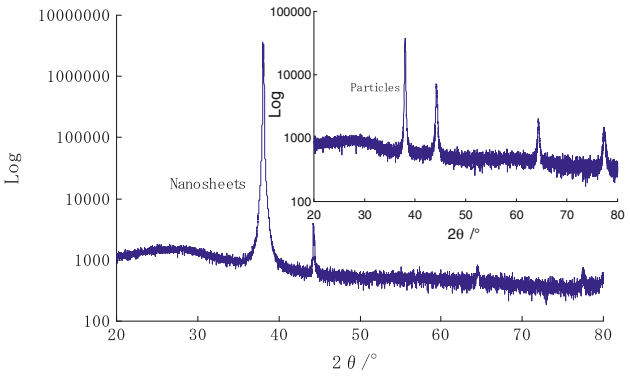

Fig. 2 XRD pattern of the Au nanosheets and Au nanoparticle (*inset*)

{111}, {200}, {220}, and {311} planes of face-centered cubic (fcc) Au (JCPDS 04-0784), respectively. This indicated pure crystalline Au was formed with the $FeCl_3$ additive. From Fig. 2, the relative (200)/(111) diffraction intensity was very low, compared with that for commercially available Au nanoparticles (inset figure). The values were 0.0011, 0.19, and 0.33 for Au nanosheets, Au nanoparticles and the standard file (JCPDS 04-0784), respectively. This indicated that the Au nanosheets predominantly contained {111} planes, and these planes were preferentially oriented parallel to the surface of the supporting substrate.

TEM and selected-area electron diffraction (SAED) patterns were used to characterize the morphology and crystallinity of the nanosheets. TEM observations were similar to those obtained with SEM. Figure 3a–c shows typical TEM images of truncated triangular, hexagonal, and triangular Au nanosheets. A selected-area electron diffraction pattern from one of the triangular nanosheet is shown in Fig. 3d. The indexing of the pattern is consistent with fcc gold oriented along a [111] axis, which agreed with the XRD results above. Sharp spots represent the (02-2), (2-20), and (202) lattice planes, in Similar results were obtained from the other shaped nanosheets. Such

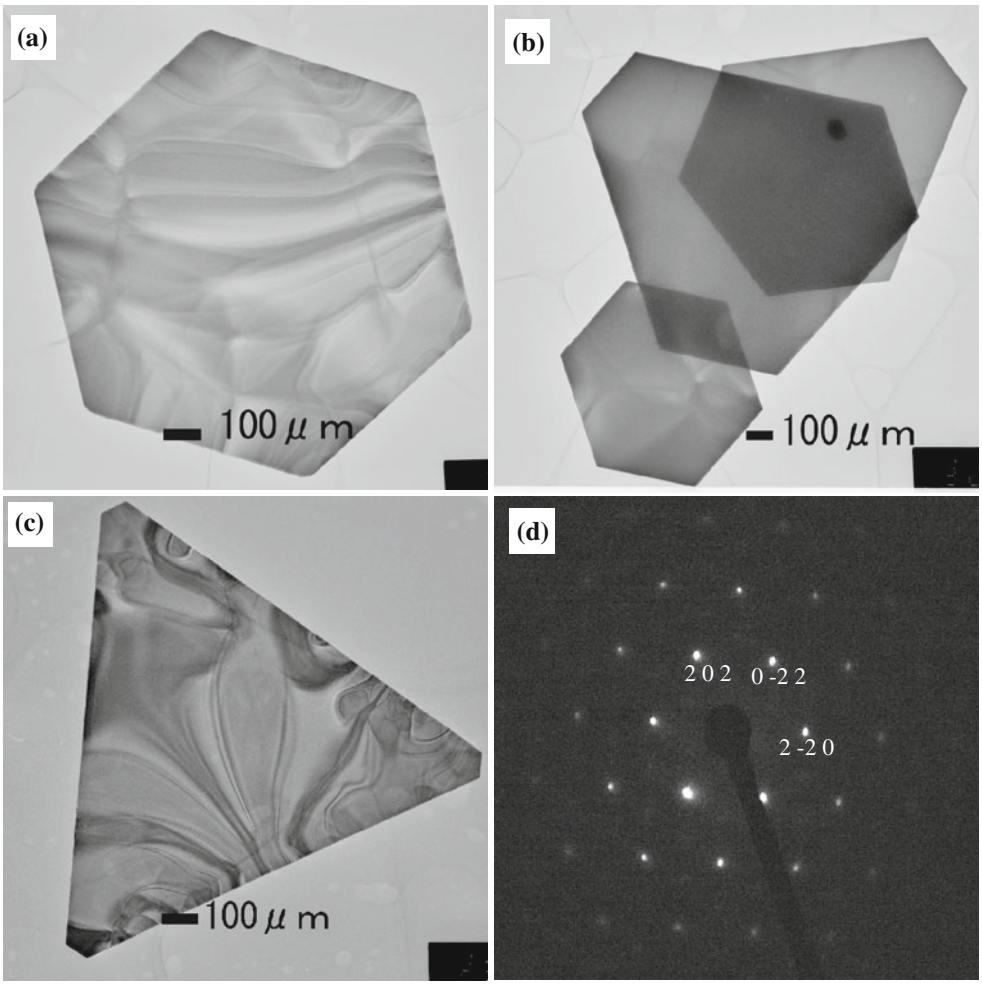

Fig. 3 Representative TEM images of nanosheets with different morphologies (**a–c**) and the electron diffraction pattern of a truncated triangular gold nanosheets (**d**). The *bar scale* is 100 nm

preferential orientation was indicative of the faceted Au particle morphology and their inherent anisotropy. Striped contrast areas in Fig. 3c reflected the buckling of Au sheets, which was attributed to internal stress as previously reported [18, 23].

In agreement with results from Li et al. [18], Au nanosheet yield and shape were dependent on PVP and $HAuCl_4 \cdot 3H_2O$ concentration and their molar ratio. Figure 4 shows typical SEM images obtained for a $HAuCl_4 \cdot 3H_2O$ concentration range of 1–20 mM. For concentrations below 4 mM, only spherical Au nanoparticles were obtained (Fig. 4a), with diameters of several tens to a few hundred nanometers. For concentrations in the range of 4–5.5 mM, two-dimensional triangular or hexagonal nanosheets were formed, in addition to many spherical particles (Fig. 4b). For concentrations in the range 6–10 mM, two-dimensional triangular, truncated triangular, and hexagonal nanosheets were the predominant products. The product also included some belt-shaped particles, which were assembled from triangular particles. The average nanosheet length depended on $HAuCl_4 \cdot 3H_2O$ concentration. At low concentration, many small triangular particles of 5 μm in length were apparent alongside a few nanosheets of ~15 μm in length (Fig. 4c). Large nanosheets of over 20 μm in length were the predominant product at high $HAuCl_4 \cdot 3H_2O$ concentration (Fig. 4d). This suggested that sheet growth was related to the collision probability of small triangular Au particles at early reaction stages. Higher $HAuCl_4 \cdot 3H_2O$ concentrations may have resulted in a large number of triangular Au particles, which immediately collided to form large triangular or hexagonal particles. Conversely, lower $HAuCl_4 \cdot 3H_2O$ concentrations resulted in a greater number of smaller particles. The Au sheet growth process was similar to that reported for the formation of Ag nanoprisms [8]. While the nanosheets were main product, the yield of Au particles decreased when the concentration of $HAuCl_4 \cdot 3H_2O$ was greater than 15 mM. Under these conditions, the reaction solution was still yellow after 5 h of heating, which indicated that $AuCl_4$ ions had not been completely reduced. This suggested the PVP capping agent was necessary for the formation of the two-dimensional nanosheets, as was reported for the formation of Ag nanorods [21]. For Ag nanorods, high PVP concentration resulted in high PVP coverage on Ag particle faces, leading to isotropic growth. Conversely, low PVP concentration resulted in anisotropic growth of wide and short rods [21]. Thus, the presence of PVP modified the Ag growth morphology. The same phenomenon was apparent for Au nanosheets in the current study. When the PVP concentration was too high (i.e., low $HAuCl_4 \cdot 3H_2O$ concentration), high PVP coverage on all Au crystal faces led to isotropic growth and the formation of round particles (Fig. 4a). Increasing $HAuCl_4 \cdot 3H_2O$ concentration acted to decrease PVP coverage and resulted in the anisotropic growth of

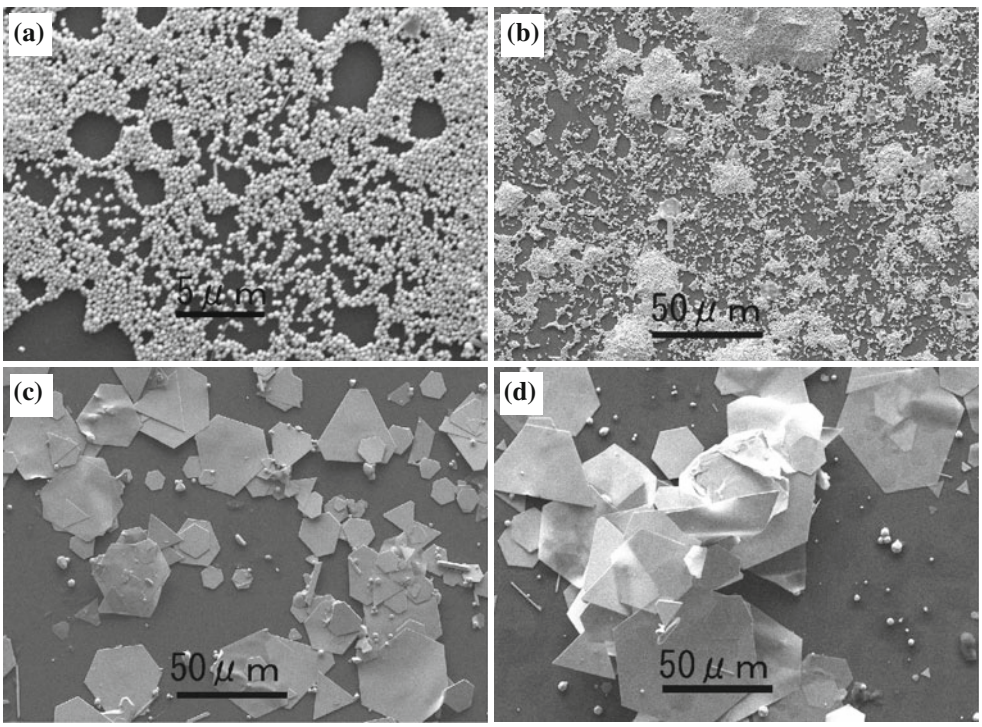

Fig. 4 Representative SEM images of Au nanoparticles prepared in 12 mL EG with 21 mg PVP and different concentration of $HAuCl_4 \cdot 3H_2O$, **a** 2 mM, **b** 5 mM, **c** 6 mM, and **d** 10 mM

large two-dimensional nanosheet particles (Fig. 4c, d). Large Au nanosheets were still the predominant product at high $HAuCl_4 \cdot 3H_2O$ concentration, which was different for the case of Ag nanorods. This implied that PVP selectively covered some Au faces in the growth process, as the process always provided some nanosheets. It also accounted for the formation of Au nanosheets at even higher PVP concentrations (Fig. 4b). Detailed reasons are still unclear.

Xia et al. reported that a very small amount of $Fe^{2+/3+}$ drastically affected the yield and shape of Ag nanowires, by removing oxygen from the surface of Ag seeds and preventing dissolution of Ag nuclei [19]. Previously, we have also found that the addition of $FeCl_3$ and other salts affected the morphology and yield of Ag nuclei in the polyol process [21]. These experiments incorporating different salts suggested that the main reason for Ag nanorod formation was anionic species, such as Cl^-, CO_3^{2-}, NO_3^{2-}, SO_4^{2-}, as opposed to metal cations. It was expected that Ag nanorod formation was closely related to the dissolution of Ag_xA_y (A = anion), which was formed following salt addition. The dissolution, i.e., the etching of Ag nuclei by anions at selected faces may also have resulted in anisotropic growth. We pondered whether Au nanosheets could be similarly formed by addition of these salts, and observed that Au nanosheet yield and shape were dramatically affected by the addition of $FeCl_3$, NaCl, and $CuCl_2$. To examine this effect in more detail, Au nanosheets were synthesized by a procedure similar to the standard synthesis using various $HAuCl_4 \cdot 3H_2O$ concentrations and constant PVP and $FeCl_3$ concentrations of 15.8 mM and 20 μM, respectively. Figure 5 shows typical SEM images obtained using a $HAuCl_4 \cdot 3H_2O$ concentration in the range of 1–20 mM. Au nanosheet formation was independent of $HAuCl_4 \cdot 3H_2O$ concentration and PVP/$HAuCl_4 \cdot 3H_2O$ molar ratio (Fig. 5a–d). It was earlier detailed how a high PVP coverage on the Au particles will result in round Au particles (Fig. 4a), and we were intrigued that the addition of $FeCl_3$ resulted in nanosheets (Fig. 5a). One possible reason is that salt ions modified Au nuclei in the early stages of growth, and facilitated assembly of nuclei into sheet-shaped particles with aid of the PVP capping agent. We were unable to find evidence for oxidative dissolution upon salt addition, as was reported for Ag nanorods [20, 21], and this implied that salt may have a further function. In Fig. 4a and b, the high PVP concentration resulted in a large barrier to anisotropic growth of Au particles. $FeCl_3$ may have decreased this PVP barrier by preferential adsorption of salt on Au faces, or by reaction between salt and PVP. Detailed reasons remain unclear. Similarly, NaCl and $CuCl_2$ salts can give same results as that of $FeCl_3$ salts. The typical SEM images are shown in Fig. 6. Although with a large amount of capping agent of PVP (15.8 M in concentration), the main product was still Au nanosheets. However, we have found that the

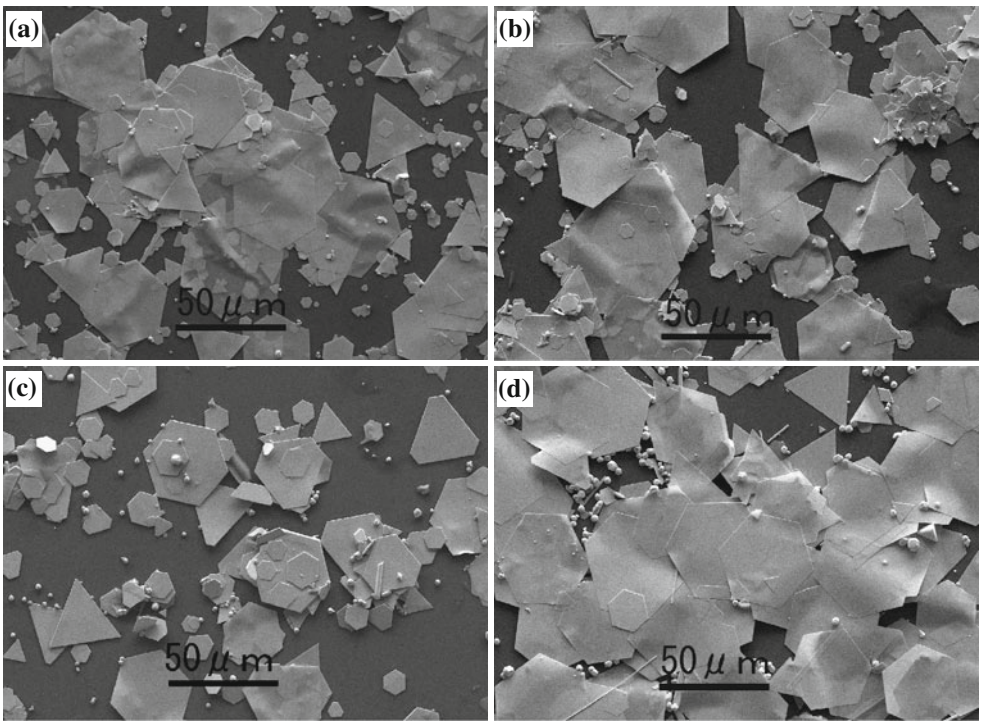

Fig. 5 Representative SEM images of nanosheets prepared with 15.8 M PVP and 20 μM $FeCl_3$ under different concentration of $HAuCl_4 \cdot 3H_2O$, **a** 2 mM, **b** 5 mM, **c** 6 mM, and **d** 10 mM

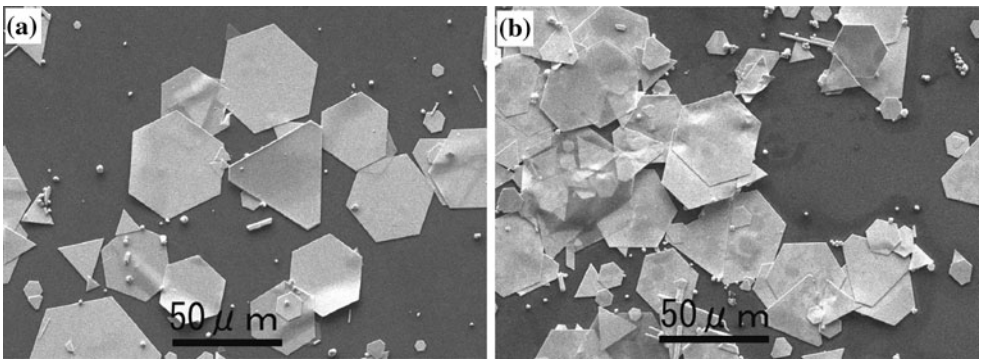

Fig. 6 Representative SEM images of nanosheets prepared with 15.8 M PVP and 5 mM $HAuCl_4 \cdot 3H_2O$ under additive of 30 μM $CuCl_2$ (**a**) and 70 μM NaCl (**b**)

concentration of used salt was different from in the case of $FeCl_3$ salt. Here, 30 μM of $CuCl_2$ (Fig. 6a) and 70 μM of NaCl (Fig. 6b) were necessary for the formation of nanosheets, which maybe implied that the important of these anionic ions, i.e., Cl^-.

We also investigated the concentration effect of salts on Au nanosheet morphology. Figure 6 shows SEM images of products synthesized using a procedure similar to the standard method. The concentrations of $HAuCl_4 \cdot 3H_2O$ and PVP were 5 and 15.8 mM, respectively. The $FeCl_3$ and NaCl concentrations were 15.6 and 32 μM (Fig. 7a, b) and 30 and 150 μM (Fig. 7c, d). The solution was reacted at 150 °C for 2 h until the color had completely disappeared. In the case of $FeCl_3$, the major product was spherical Au nanoparticles and a small amount of nanosheets (Fig. 4b) without $FeCl_3$. When $FeCl_3$ (15.6 μM) was added, the spherical particle content drastically decreased and was substituted for a large amount of sheet-shaped particles and a lesser amount of belt-shaped particles (Fig. 7a). The yield of spherical particles was lower than 20%. Following centrifugation, the supernatant was colorless and a broad asymmetric peak was evident at ~560 nm in the UV–vis absorption spectra. This indicated that large particles and sheet-like particles were both present [9, 24]. When the $FeCl_3$ concentration was increased to 20 μM, two-dimensional nanosheets became the main product (Fig. 5b). Further increasing $FeCl_3$ concentration to 32 μM resulted in sheets still being the main product, and a small quantity

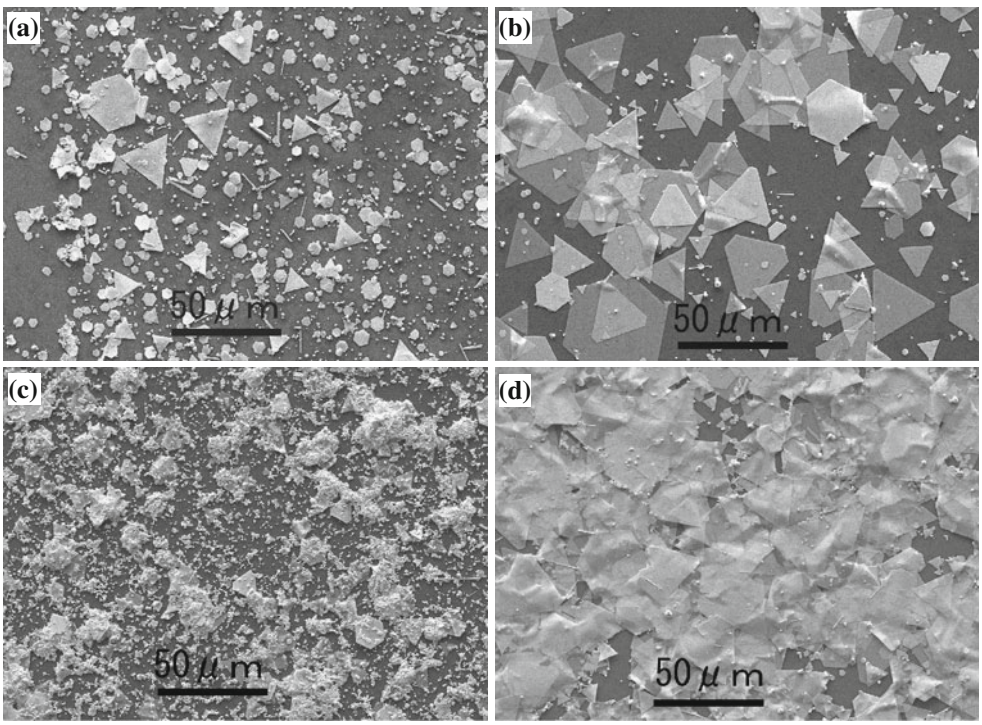

Fig. 7 SEM images of Au nanosheets prepare with 5 M PVP and 15.8 M $HAuCl_4 \cdot 3H_2O$ at $FeCl_3$ concentration of **a** 15.6 and **b** 32 μM, and NaCl concentration of **c** 20 and **d** 150 μM

of round particles (Fig. 7b). Similar results have been obtained with NaCl salt. When the concentration NaCl was 20 μM, the product was a mixture of spherical, sheet-shaped, and belt-shaped particles (Fig. 7c). When the concentration of NaCl was increased, the spherical particles content decreased and was substituted for a large amount of sheet-shaped particles (Fig. 6b). Further increasing the concentration to 150 μM, the main product was sheet-shaped particles including a small amount of spherical particles (Fig. 7d).

In our previous reports about Ag nanorod fabrication [21], the addition of other salts including NaCl, $ZnCl_2$, $NiCl_2$, $CoCl_2$, $CuCl_2$, Na_2CO_3, Na_2S, $NiCO_3$, and Na_2SO_4 were all found to result in Ag nanorods. The formation of Ag nanorods was found to depend on the dissolution of Ag_xA_y (A = anion), which was formed following salt addition, or by the etching of Ag nuclei from anions. The hypothesis came from the decreasing of Ag nuclei after these salts have been added in the reaction solution. In the current study, we also attempted to prepare Au nanosheets using these salts. Similar results have been obtained. Au nanosheets have been obtained with these salt additives, such as $FeCl_3$, NaCl, and $CuCl_2$ salt additives. The difference was that reducing phenomenon of Au concentration was not observed in the formation of Au nanosheets, which implied that the salt additives may play other roles. On the other hand, an experiment with 5 mM of $HAuCl_4{\cdot}3H_2O$ and 32 μM of $FeCl_3$ with no PVP also had been carried out. Some sheet-shaped Au particles were formed in agglomerated states, which suggested PVP was necessary for the formation of independent Au nanosheets. With salt and $HAuCl_4{\cdot}3H_2O$ only, no sheet-shaped Au particles could be formed from the polyol process. The function of salt may be related to adsorption and coverage on the Au nuclei surface. The effect of PVP and salt ions on the Au surface facilitates their assembly into sheet-shape particles. However, there is no direct evidence for the adsorption or dissolution function of salts in the present study, which should be carefully studied to understand the growth mechanism of anisotropic metal particles in the polyol process.

Conclusions

Triangular and hexagonal single-crystalline Au nanosheets were synthesized on a large scale, by the polyol process in ambient atmospheric conditions. The reduction of $HAuCl_4{\cdot}3H_2O$ in EG with a small amount of PVP capping agent and salts was carried out. The formation of nanosheets was found to be independent of the concentration of $HAuCl_4{\cdot}3H_2O$ in the presence of salts. The existence of PVP and salt ions on Au faces improved the growth of Au particles and facilitated their assembly into sheet-shaped particles. These results suggest metal particles of other morphologies could be prepared with careful salt and capping agent selection.

Acknowledgements The authors are grateful to Prof. S. Isoda for helpful discussions. We thank Dr. T. Nemoto and Dr. R. Kozawa for assistance with TEM measurements. This work was part of the Development of Inverter Systems for Power Electronics project, supported by the New Energy and Industrial Technology Development Organization.

References

1. Roucoux A, Schulz J, Patin H (2002) Chem Rev 102:3757
2. Mulvaney SP, Musick MD, Keating CD, Natan M (2003) J Langmuir 19:4784
3. Song Y, Medforth CJ, Pereira E, Singh AK, Xu H, Jiang Y, Brinker J, Swol FV, Shelnutt JA (2004) J Am Chem Soc 126:635
4. Chen J, Wiley BJ, Xia Y (2007) Langmuir 23:4120
5. Bradley JS, Tesche B, Busser W, Maase M, Reetz MTA (2000) J Am Chem Soc 122:4631
6. Jin R, Cao Y, Mirkin CA, Kelly KL, Schatz GC, Zheng J (2001) Science 294:1901
7. Chen S, Carroll DL (2002) Nano Lett 2:1003
8. Jin R, Cao Y, Hao E, Metraux GS, Schatz GC, Mirkin CA (2003) Nature 425:487
9. Sun X, Dong S, Wang E (2004) Angew Chem Int Ed 43:6360
10. Kim J, Cha S, Shin K, Jho JY, Lee JC (2004) Adv Mater 16:459
11. Wang L, Chen X, Zhan J, Chai Y, Yang C, Xu L, Zhuang W, Jing B (2005) J Phys Chem B 109:3189
12. Ahmadi TS, Wang ZL, Green TC, Henglein A, El-Sayed MA (1996) Science 272:1924
13. Sun Y, Xia Y (2002) Science 298:2176
14. Attard GS, Bartlett PN, Coleman NRB, Elliott JM, Owen JR, Wang JH (1997) Science 278:838
15. Zhao DY, Feng JL, Huo QS, Melosh N, Fredrickson GH, Chmelka BK, Stucky GD (1998) Science 279:548
16. Fischer C, Heller A, Dube G (1989) Mat Res Bull 24:1271
17. Tsuji M, Hashimoto M, Nishizawa Y, Tsuji T (2003) Chem Lett 32:1114
18. Li C, Cai W, Cao B, Sun F, Li Y, Kan C, Zhang L (2006) Adv Funct Mater 16:83
19. Willey B, Sun Y, Xia Y (2005) Langmuir 21:8077
20. Willey B, Herricks T, Sun Y, Xia Y (2004) Nano Lett 4:1733
21. Jiu J, Murai K, Kim D, Kim K, Suganuma K (2009) Mater Chem Phys 114:333
22. Chen J, Herricks T, Geissler M, Xia Y (2004) J Am Chem Soc 126:10854
23. Tetsuya K (2008) Langmuir 24:7648
24. Wang L, Chen X, Zhan J, Sui Z, Zhao J, Sun Z (2004) Chem Lett 33:720